



FLUSH-MOUNTED DIELECTRIC-LOADED AXIAL SLOT
ON CIRCULAR CYLINDER

J. H. Richmond

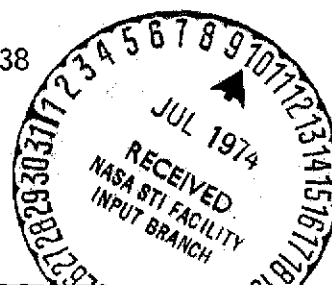
The Ohio State University
ElectroScience Laboratory

Department of Electrical Engineering
Columbus, Ohio 43212

TECHNICAL REPORT 2902-17

Grant Number NGL 36-008-138

June 1974



(NASA-CR-138752) FLUSH-MOUNTED
DIELECTRIC-LOADED AXIAL SLOT ON CIRCULAR
CYLINDER (Ohio State Univ.) 34 p HC
\$4.75

N74-27619

CSCI 20N

Unclas

G3/07 42480

National Aeronautics and Space Administration
Langley Research Center
Hampton, Va. 23365

NOTICES

When Government drawings, specifications, or other data are used for any purpose other than in connection with a definitely related Government procurement operation, the United States Government thereby incurs no responsibility nor any obligation whatsoever, and the fact that the Government may have formulated, furnished, or in any way supplied the said drawings, specifications, or other data, is not to be regarded by implication or otherwise as in any manner licensing the holder or any other person or corporation, or conveying any rights or permission to manufacture, use, or sell any patented invention that may in any way be related thereto.

FLUSH-MOUNTED DIELECTRIC-LOADED AXIAL SLOT
ON CIRCULAR CYLINDER

J. H. Richmond

TECHNICAL REPORT 2902-17

Grant Number NGL 36-008-138

June 1974

National Aeronautics and Space Administration
Langley Research Center
Hampton, Va. 23365

ABSTRACT

This report presents the theory, computer program and numerical results for an axial slot antenna on a circular cylinder.

CONTENTS

	Page
I. INTRODUCTION	1
II. THEORY	1
III. NUMERICAL RESULTS	7
IV. SUMMARY AND CONCLUSIONS	13
REFERENCES	14
APPENDIX I - THE MAIN COMPUTER PROGRAM	15
APPENDIX II - SUBROUTINE BESSI	20
APPENDIX III - SUBROUTINE SQROT	29
ACKNOWLEDGMENT	30

I. INTRODUCTION

We consider an axial slot antenna on a perfectly conducting circular cylinder. The cylinder is partially coated with a dielectric layer, and the antenna radiates through this flush-mounted window. The motivation for this study is to determine the effects of a high-temperature dielectric layer on the performance of antennas mounted on a space shuttle.

For an axial slot antenna on a circular cylinder completely coated with a dielectric layer, the admittance and patterns have been investigated by Knop[1], Fante[2], and Croswell, Westrick and Knop[3]. Our analysis has some similarity to that of Billingsley and Sinclair[4] for scattering by circular-sector cylinders.

The following sections define the problem and present the theory, computer programs and some numerical results.

II. THEORY

Consider an axial slot antenna on a perfectly conducting circular cylinder as illustrated in Fig. 1. The inner aperture has radius "a" and

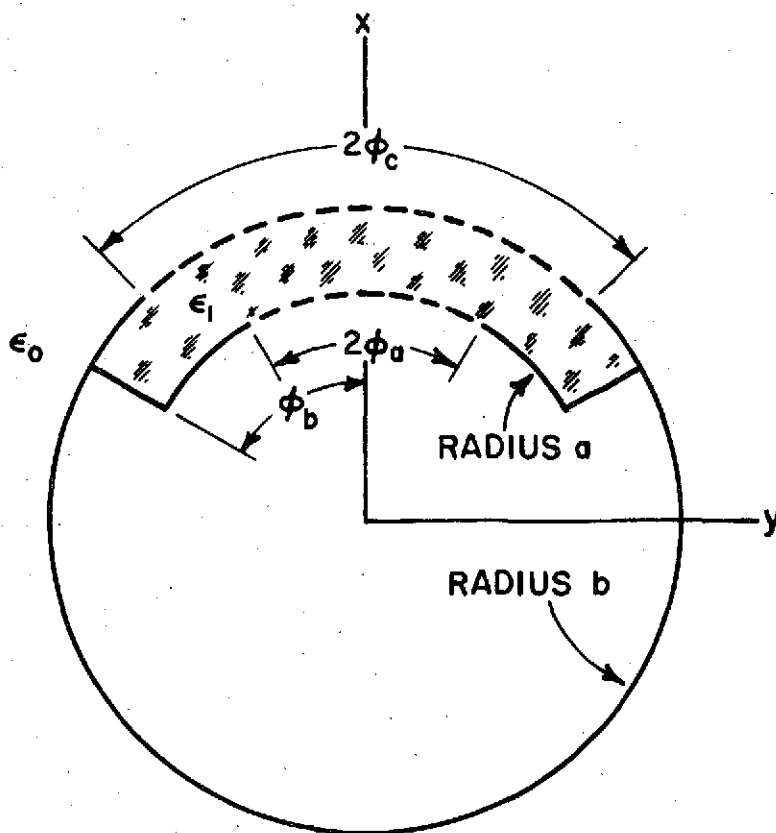


Fig. 1. An axial-slot antenna radiates through a flush-mounted dielectric window in a conducting circular cylinder.

half-angle ϕ_a . The outer aperture has radius b and half-angle ϕ_c . The exterior medium is free space. The inner slot radiates through a flush-mounted homogeneous dielectric window with permittivity ϵ_1 , permeability μ_1 , inner radius a , outer radius b and half-angle ϕ_b . The metallic flange prevents the dielectric window from falling out. This cylindrical structure has infinite length, and its axis coincides with the z axis. We consider a time-harmonic excitation with the time dependence $e^{j\omega t}$ understood, and the fields have no z dependence. This report considers the TE polarization in which the non-zero field components are E_ρ , E_ϕ and H_z . Given an even field distribution E_ϕ over the inner aperture, the objective is to determine the aperture admittance, gain and far-field pattern of this antenna. Our solution employs cylindrical-mode expansions and Galerkin's method.

The field in region I (the dielectric window) is

$$(1) \quad E_\rho^I = \frac{j\eta_1}{k_1 \rho} \sum_k v [c_k J_v(\rho) + d_k N_v(\rho)] \sin v\phi$$

$$(2) \quad E_\phi^I = j\eta_1 \sum_k [c_k J'_v(\rho) + d_k N'_v(\rho)] \cos v\phi$$

$$(3) \quad H_z^I = \sum_k [c_k J_v(\rho) + d_k N_v(\rho)] \cos v\phi$$

$$(4) \quad k_1 = \omega \sqrt{\mu_1 \epsilon_1}$$

$$(5) \quad \eta_1 = \sqrt{\mu_1 / \epsilon_1}$$

$$(6) \quad v = k\pi / \phi_b$$

where the integer k runs from zero to infinity and (ρ, ϕ, z) are the cylindrical coordinates. (In this report the symbols $J_v(\rho)$ and $N_v(\rho)$ denote the Bessel and Neumann functions with order v and argument $k_1 \rho$.) This field satisfies the source-free version of Maxwell's equations in region I. From Eqs. (1) and (6), tangential E vanishes at the perfectly conducting surfaces at $\phi = \pm \phi_b$. The expansion constants c_k and d_k are to be determined from the boundary conditions.

The voltage across the inner aperture is

$$(7) \quad V = 2a \int_0^{\phi_a} E \, d\phi$$

where E denotes $E_\phi(a, \phi)$. (We assume the aperture field E is a specified even function of ϕ .) The external admittance of the inner aperture is

$$(8) \quad Y = \frac{2a}{VV^*} \int_0^{\phi_a} E^* H_Z^I(a, \phi) \, d\phi.$$

The boundary condition at $\rho = a$ is

$$(9) \quad E_\phi^I = \begin{cases} E & \text{for } 0 < \phi < \phi_a \\ 0 & \text{for } \phi_a < \phi < \phi_b \end{cases}.$$

From Eqs. (2) and (9) with Fourier analysis,

$$(10) \quad j\eta_1 \phi_b [c_k J'_v(a) + d_k N'_v(a)] = e_k G_k$$

$$(11) \quad G_k = \int_0^{\phi_a} E \cos v\phi \, d\phi$$

where $e_0 = 1$ and $e_k = 2$ for $k = 1, 2, 3, \dots$

From Eqs. (3) and (8), the external admittance (per unit length of cylinder) of the inner aperture is

$$(12) \quad Y = \frac{2a}{VV^*} \sum_k [c_k J_v(a) + d_k N_v(a)] G_k^*.$$

The field in region II (the exterior free-space region) is

$$(13) \quad E_\rho^{II} = \frac{j\eta_0}{k_0 \rho} \sum_i i a_i H_i(\rho) \sin i\phi$$

$$(14) \quad E_\phi^{II} = j\eta_0 \sum_i a_i H'_i(\rho) \cos i\phi$$

$$(15) \quad H_z^{II} = \sum_i a_i H_i(\rho) \cos i\phi$$

$$(16) \quad k_0 = \omega \sqrt{\mu_0 \epsilon_0}$$

$$(17) \quad n_0 = \sqrt{\mu_0 / \epsilon_0}$$

where the integer i runs from zero to infinity. (In this report the symbol $H_i(\rho)$ denotes the Hankel function with order i and argument $k_0\rho$ and the superscript (2) is understood. The argument $k_1\rho$ will not be encountered with the Hankel function.) This field satisfies the radiation conditions and the source-free version of Maxwell's equations.

To complete the solution, it remains only to enforce the boundary conditions at $\rho = b$. The rigorous solution involves an infinite system of simultaneous linear equations. We desire an accurate approximation involving a finite system of simultaneous linear equations. To develop a solution of this type, we expand the field in the outer aperture (at $\rho = b$) as follows:

$$(18) \quad E_\phi = \sum_n b_n \cos(n\pi\phi/\phi_c) \quad \text{for } 0 < \phi < \phi_c$$

where n runs from zero to N . If the constants b_n were known, the remaining constants (a_i , c_k and d_k) could be determined. In this sense the b_n are independent unknowns, and the others are dependent. When the simultaneous linear equations are written as a matrix equation, the square matrix will be symmetric if the b_n are chosen as the independent quantities.

From Eq. (2) and the boundary condition on E_ϕ^I at $\rho = b$,

$$(19) \quad j\eta_1 \sum_k [c_k J'_v(b) + d_k N'_v(b)] \cos v\phi = \begin{cases} E_\phi & \text{for } 0 < \phi < \phi_c \\ 0 & \text{for } \phi_c < \phi < \phi_b \end{cases}$$

where E_ϕ is defined by Eq. (18). Multiplying both sides of Eq. (19) by $\cos v\phi$ and integrating over the range $0 < \phi < \phi_b$ yields

$$(20) \quad j\eta_1 \phi_b [c_k J'_v(b) + d_k N'_v(b)] = e_k \sum_n b_n F_{kn}$$

$$(21) \quad F_{kn} = \int_0^{\phi_c} \cos(k\pi\phi/\phi_b) \cos(n\pi\phi/\phi_c) d\phi.$$

From Eqs. (10) and (20),

$$(22) \quad c_k = P_k \left[G_k N'_v(b) - N'_v(a) \sum_n b_n F_{kn} \right]$$

$$(23) \quad d_k = P_k \left[-G_k J'_v(b) + J'_v(a) \sum_n b_n F_{kn} \right]$$

$$(24) \quad P_k = \frac{e_k}{jn_1 \phi_b [J'_v(a) N'_v(b) - J'_v(b) N'_v(a)]}$$

From Eq. (14) and the boundary condition on E_ϕ^{II} at $\rho = b$,

$$(25) \quad jn_0 \sum_i a_i H'_i(b) \cos i\phi = \begin{cases} E_\phi & \text{for } 0 < \phi < \phi_c \\ 0 & \text{for } \phi_c < \phi < \pi \end{cases}$$

where E_ϕ is defined by Eq. (18). Multiplying both sides of Eq. (25) by $\cos i\phi$ and integrating over the range $0 < \phi < \pi$ yields:

$$(26) \quad a_i = \frac{e_i}{j\pi n_0 H'_i(b)} \sum_n b_n G_{in}$$

$$(27) \quad G_{in} = \int_0^{\phi_c} \cos(i\phi) \cos(n\pi\phi/\phi_c) d\phi.$$

Equations (22)-(26) show explicitly that a knowledge of the constants b_n is sufficient to determine all the other constants.

At this point we have used the boundary conditions on E_ϕ to relate a_i , c_k and d_k to b_n . The next step is to use the boundary condition on H_z to generate a system of simultaneous linear equations for the constants b_n . From Eqs. (3) and (15) and continuity of tangential H across the outer aperture (at $\rho = b$):

$$(28) \quad \sum_i a_i H_i(b) \cos i\phi = \sum_k [c_k J_v(b) + d_k N_v(b)] \cos v\phi$$

where ϕ ranges from zero to ϕ_c . In Eq. (28), multiplying both sides by $\cos(m\pi\phi/\phi_c)$ and integrating from $\phi = 0$ to $\phi = \phi_c$ yields

$$(29) \quad \sum_i a_i H_i(b) G_{im} = \sum_k [c_k J_v(b) + d_k N_v(b)] F_{km}.$$

In matching H_z across the aperture, we selected the same weighting function $\cos(m\pi\phi/\phi_c)$ also used as a basis function in Eq. (18). This is the distinctive feature of Galerkin's method. If Eqs. (22), (23) and (26) are used to eliminate a_i , c_k and d_k , Eq. (29) yields:

$$(30) \quad \sum_n Z_{mn} b_n = V_m \quad \text{with } m = 0, 1, 2, \dots, N$$

$$(31) \quad V_m = \frac{2 j \eta_1 \phi_b}{k_1 b \phi_c} \sum_k P_k G_k F_{km}$$

$$(32) \quad Z_{mn} = \frac{\phi_b}{\phi_c} \left[\frac{\eta_1}{\eta_0} \sum_i \frac{e_i H_i(b) G_{im} G_{in}}{H_i'(b)} + \frac{\pi}{\phi_b} \sum_k e_k R_k F_{km} F_{kn} \right]$$

$$(33) \quad R_k = \frac{J_v(b) N_v'(a) - J_v'(a) N_v(b)}{J_v'(a) N_v'(b) - J_v(b) N_v'(a)}.$$

Equation (30) is recognized as a system of simultaneous linear equations. In the summation, n runs from zero to N . Equation (30) can also be written as a matrix equation. The symmetry of the square matrix Z_{mn} is obvious in Eq. (32).

The matrix equation is solved with a digital computer to obtain numerical values for b_n . Then Eqs. (22), (23) and (26) are employed to determine c_k , d_k and a_i . The aperture admittance is obtained from Eq. (12). The far-field pattern is obtained from Eq. (15) as follows:

$$(34) \quad H_z = e^{-jk\rho} \sqrt{\frac{2j}{\pi k\rho}} \sum_i a_i j^i \cos i\phi.$$

The power gain is calculated as follows:

$$(35) \quad G_p(\phi) = \frac{2\pi\rho\eta_0 |H_z(\rho, \phi)|^2}{VV^*G}$$

where the aperture voltage V is given by Eq. (7) and the aperture conductance G is the real part of Y in Eq. (12).

III. NUMERICAL RESULTS

Figures 2-6 illustrate the far-field patterns of an axial slot antenna radiating through a lossless window with dielectric constant of 1, 1.2, 2, 3 and 4. Figures 2 and 3 compare the calculated patterns with experimental measurements performed at NASA Langley. Measurements are not available for the other cases. In this sequence of figures all parameters of the slot, window and cylinder are fixed except the dielectric constant. The electric field distribution is uniform across the inner aperture.

All the patterns are reasonably smooth except in Fig. 5 where the pattern breaks up into many lobes with deep nulls. With a dielectric constant of 3, this anomalous type of pattern is observed when the aperture half-angle is $\phi_b = 13.8, 14.8, 15.8, 16.8^\circ$, etc. When ϕ_b differs from one of these critical angles by more than 0.1 degrees, the pattern becomes smooth again. At each critical angle, the aperture width is an integral number of wavelengths for the lowest-order surface wave. This surface-wave resonance phenomenon is less pronounced with a dielectric constant of 1.2 but is observed when $\phi_b = 14.6^\circ$. The effect may be reduced with a lossy dielectric window or by reducing the reflection coefficient at the edges of the aperture.

In these figures, the calculations are based on a two-dimensional model with an infinitely long axial slot. A case of greater interest is a half-wave axial slot in a long cylinder. The effects of surface-wave resonance will be reduced with a slot of finite length.

In generating the data for Fig. 5, the execution time was 50 seconds on a Datacraft 6024/3 computer. The solution involved a system of 20 simultaneous linear equations ($N = 19$ in Eqs. (18) and (30)). The infinite series with index i (in Eqs. (32) and (34)) were truncated after 148 terms, and the series with index k (in Eqs. (12), (31) and (32)) were truncated after 20 terms. The calculated aperture admittance was $0.372 + j 0.122$ mhos/wavelength. Identical results were obtained with $N = 18$ and 19, but $N = 15$ proved inadequate.

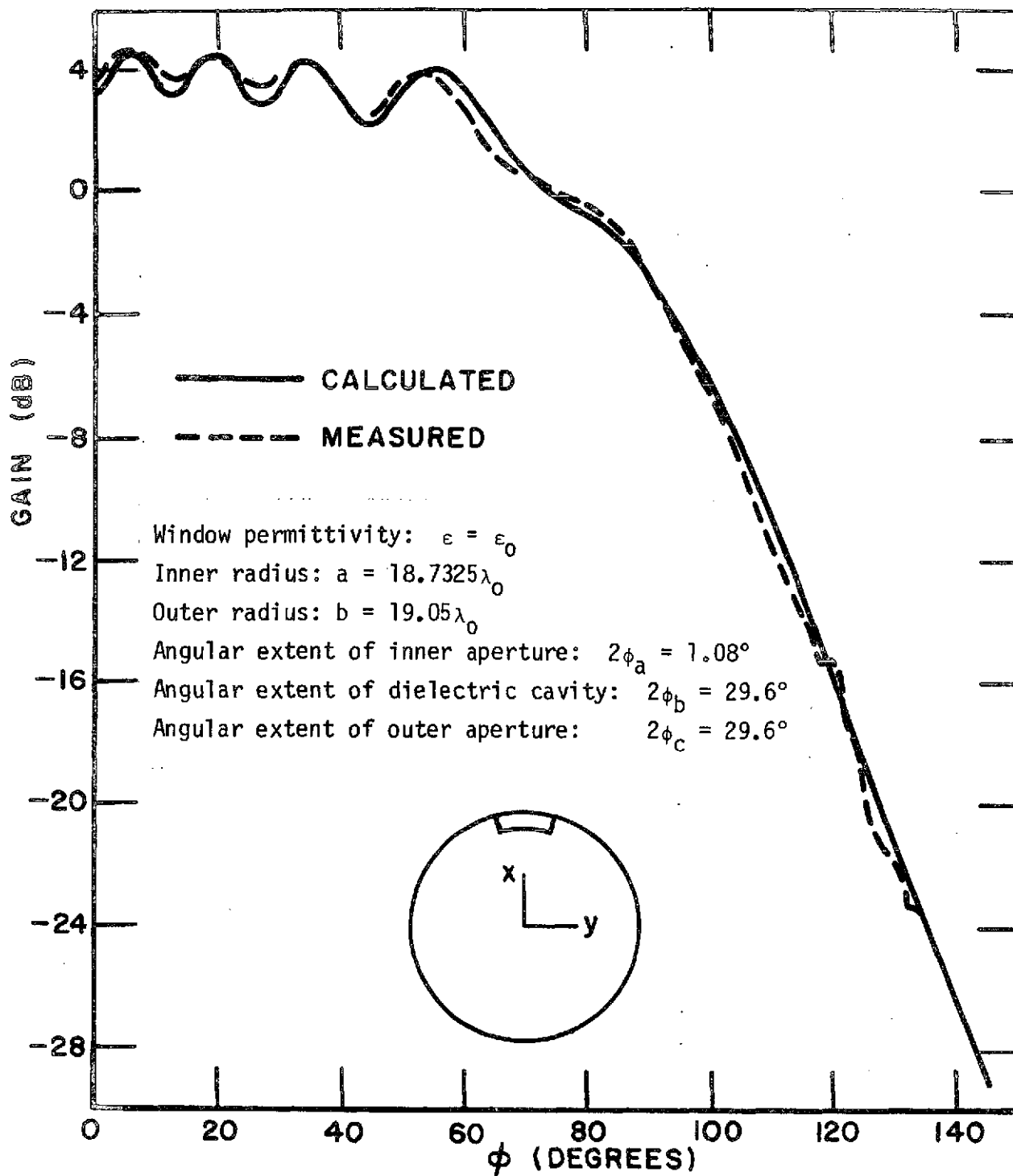


Fig. 2. Far-field pattern with $\epsilon_r = 1$.

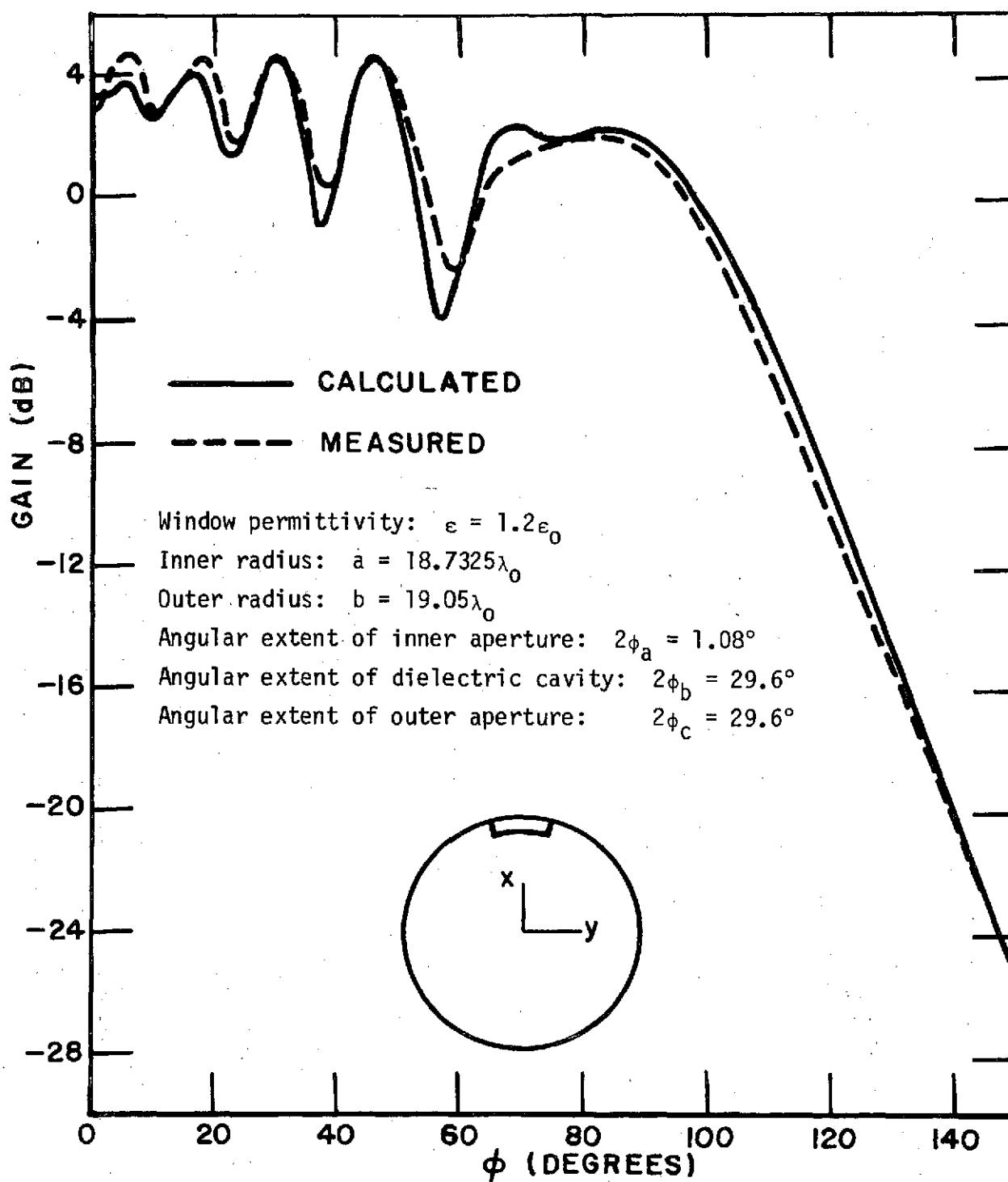


Fig. 3. Far-field pattern with $\epsilon_r = 1.2$.

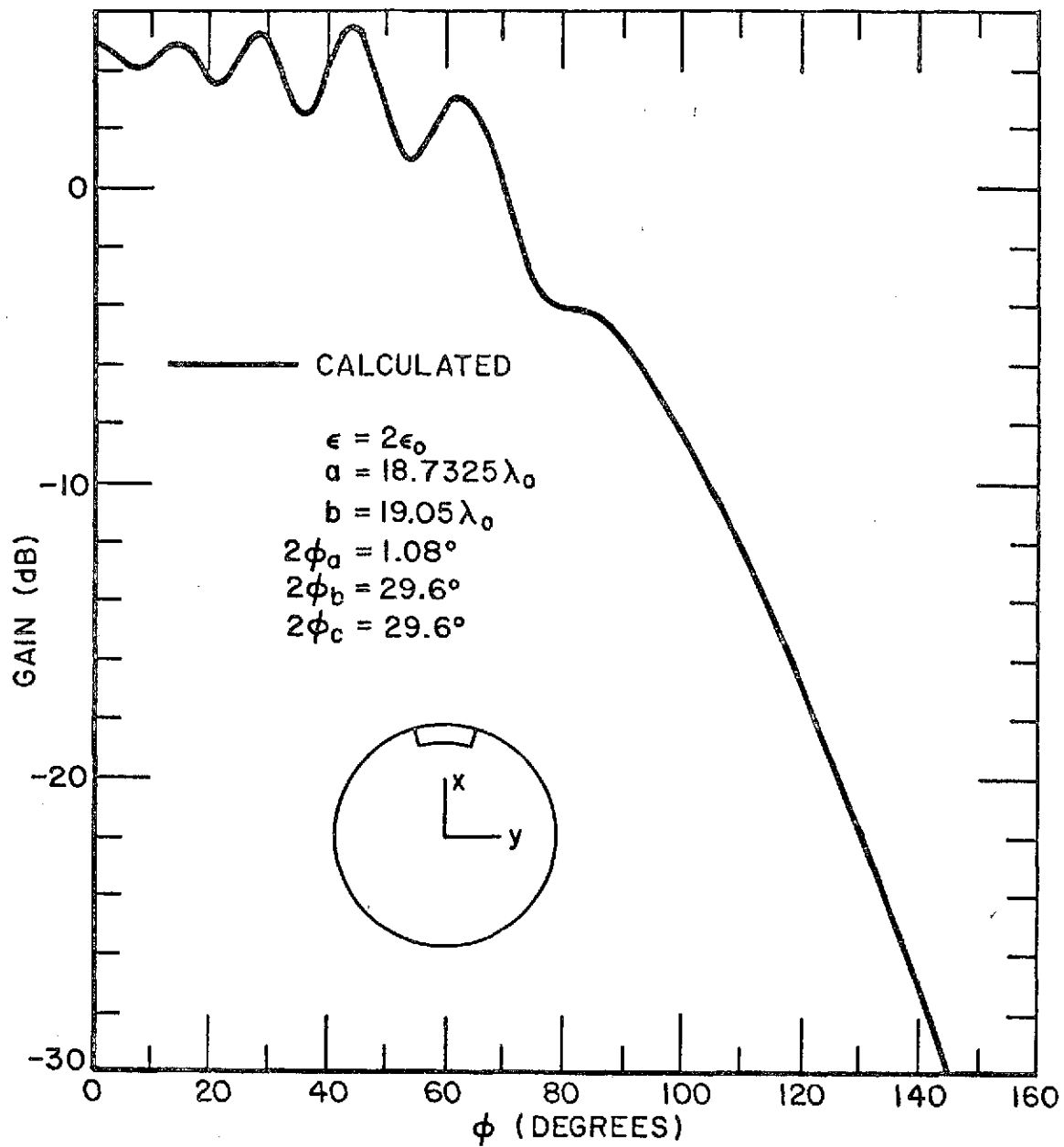


Fig. 4. Far-field pattern with $\epsilon_r = 2$.

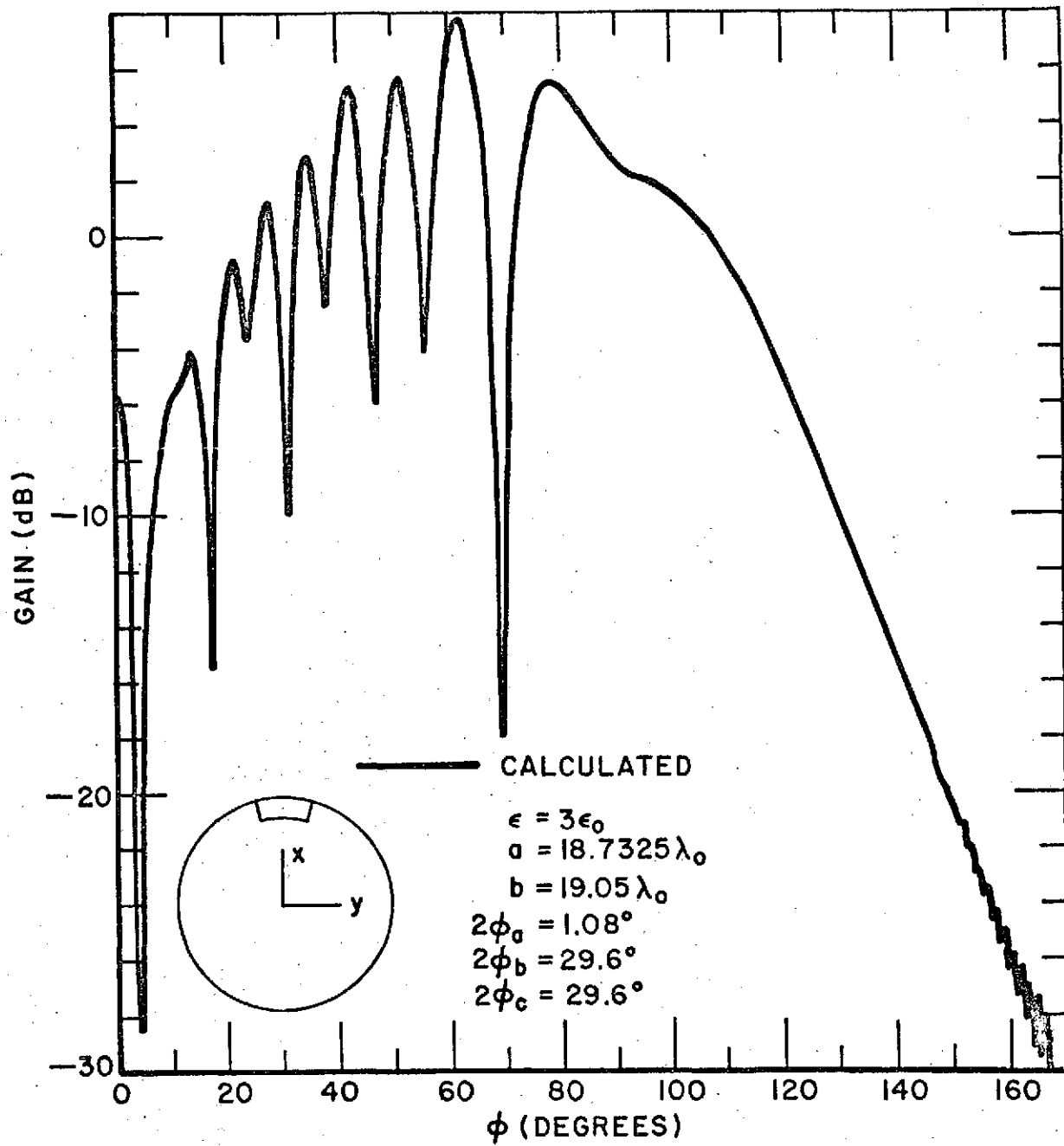


Fig. 5. Far-field pattern with $\epsilon_r = 3$.

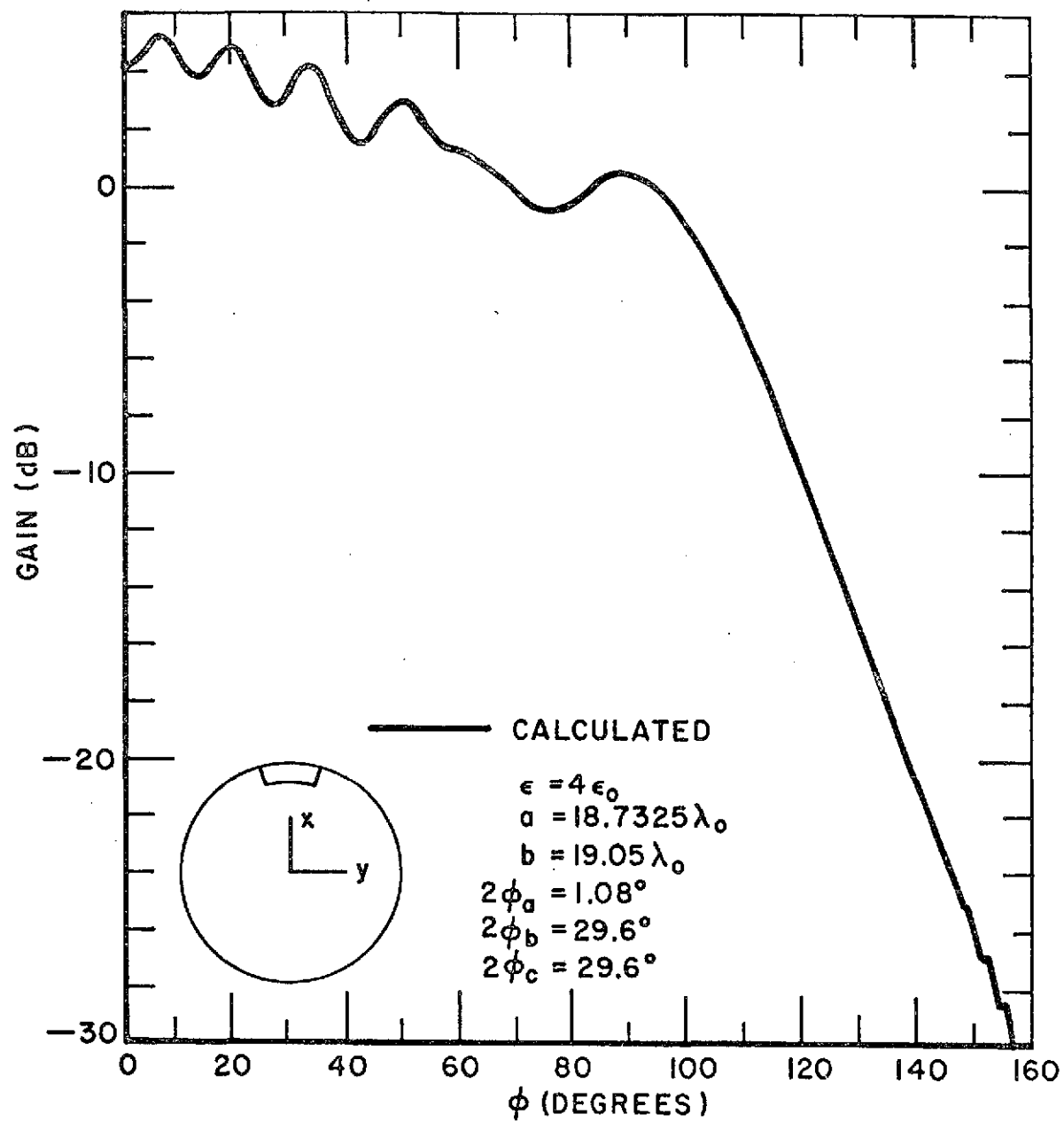


Fig. 6. Far-field pattern with $\epsilon_r = 4$.

IV. SUMMARY AND CONCLUSIONS

This report develops the theoretical formulation for a TE axial slot antenna radiating through a dielectric window in a circular cylinder. Numerical results are presented for the far-field patterns, and it is noted that the calculations show excellent agreement with experimental measurements. The computer program is presented in the Appendices.

The solution is based on Galerkin's method. Simultaneous linear equations are generated in which the unknown quantities are the coefficients in a Fourier-series expansion for the electric field in the outer aperture. The formulation is rapidly convergent, and the computer program is quite efficient.

REFERENCES

1. Knop, C.M., "External Admittance of an Axial Slot on a Dielectric Coated Metal Cylinder," Radio Science, Vol. 3, No. 8, August 1968, pp. 803-817.
2. Fante, R.L., "Calculation of the Admittance, Isolation, and Radiation Pattern of Slots on an Infinite Cylinder Covered by an Inhomogeneous Lossy Plasma," Radio Science, Vol. 6, No. 3, March 1971, pp. 421-428.
3. Croswell, W.F., Westrick, G.C. and Knop, C.M., "Computations of the Aperture Admittance of an Axial Slot on a Dielectric Coated Cylinder," IEEE Trans., Vol. AP-20, January 1972, pp. 89-92.
4. Billingsley, J.B. and Sinclair, G., "Numerical Solutions to Electromagnetic Scattering from Strips, Finite Wedges, and Notched Circular Cylinders," Canadian Journal of Physics, Vol. 44, 1966, pp. 3217-3225.
5. Goldstein, M. and Thaler, R.M., "Recurrence Techniques for the Calculation of Bessel Functions," MTAC (Mathematics of Computation) Vol. 13, April, 1959, pp. 102-108.
6. Goldstein, M. and Thaler, R.M., "Bessel Functions for Large Arguments," MTAC (Mathematics of Computation) Vol. 12, January 1958, pp. 18-26.

APPENDIX I THE MAIN COMPUTER PROGRAM

The MAIN computer program is listed in Fig. 7. In this program E_ϕ is uniform across the inner aperture and the dielectric window is lossless. Following the format statements, the dimensions are indicated for the subscripted quantities as follows:

IDC dimension of B and V
IDH dimension of A, BHR, BB, YY, BP, YP, SNC and SGA
IDJ dimension of C, D, SGC, RBES, BEN, AJJ, etc
IDZ dimension of Z.

The input data are programmed at statement 20 with the following definitions:

AL inner radius a/λ
BL outer radius b/λ
ER dielectric constant ϵ_1/ϵ_0
DPH angular increment for far-field pattern calculations
PHA ϕ_a in degrees
PHB ϕ_b in degrees
PHC ϕ_c in degrees

where λ denotes the wavelength in free space.

At statement 30, subroutine BESSI is called for the Bessel and Neumann functions and their derivatives. This subroutine also determines the number of terms (denoted by KK) to be employed in the summations on k in Eqs. (12), (31) and (32). The last call to BESSI determines the number of terms (denoted by II) to be employed in the summations on i in Eqs. (32) and (34). If KK is equal to IDJ, the dimension IDJ should be increased. If II is equal to IDH, the dimension IDH should be increased. II should exceed IMIN, and KK should exceed KMIN. NN denotes the number of simultaneous linear equations and the number of terms to be employed in the summations on n in Eqs. (22), (23) and (26). NN should exceed NMIN.

For a uniform aperture distribution with $V = 1$ volt, Eqs. (7) and (11) yield

$$(36) \quad G_k = \frac{\sin(v\phi_a)}{2av\phi_a}.$$

In the computer program, SGA(K) denotes $2aG_k$. Subroutine GLJ calculates F_{kn}/ϕ_c where F_{kn} is defined by Eq. (21). Subroutine GNJ calculates

G_{in}/ϕ_c where G_{in} is defined by Eq. (27). Some of the symbols used in the program are defined as follows:

A	a_i
B	b_n/k_o
C	c_k
D	d_k
V	v_m/k_o
AK	$k_o a$
BK	$k_o b$
AK1	$k_1 a$
BK1	$k_1 b$
BEN	denominator in Eq. (33)
BHR	$H_i(b)/H_1'(b)$
ETA	η_o
ETA1	η_1
GNU	v
RBES	$-R_k$
SGC	$(\sin v\phi_c)/(v\phi_c)$
SNC	$(\sin i\phi_c)/(i\phi_c)$
SJN	first summation in Eq. (32)
SJL	second summation in Eq. (32)
Y11	aperture admittance Y
Z(L)	Z_{mn}

In statement 130, subroutine SQROT is called to solve the system of simultaneous linear equations. Then the expansion coefficients a_i , c_k and d_k are calculated from Eqs. (22), (23) and (26). The aperture admittance is calculated at statement 360 with Eq. (12). Finally, the gain is calculated with Eqs. (34) and (35).

C	TE AXIAL SLOT IN PERFECTLY CONDUCTING CIRCULAR CYLINDER.	0001
C	SLOT RADIATES THROUGH DIFLECTRIC WINDOW.	0002
C	PROGRAM BY JACK H RICHMOND, OHIO STATE UNIVERSITY.	0003
	COMPLEX V(30),R(30),Z(465),C(150),D(150),A(400),HHR(400)	0004
	COMPLEX CQ,HZ,SUMN,SUL,SJN,Y11	0005
	DIMENSION BB(400),YY(400),BP(400),YP(400),SNC(400),SGA(400)	0006
	DIMENSION SGC(150),RBES(150),BEN(150)	0007
	DIMENSION AJJ(150),AYY(150),AJP(150),AYP(150)	0008
	DIMENSION BJ1(150),BY1(150),BJP1(150),BYP1(150)	0009
	EQUIVALENCE (B,V),(BB,SNC),(YY,SGA),(BJ1,SGC),(BY1,RBES)	0010
	DATA ETA,PI,TP/376.727,3.14159,6.28318/	0011
2	FORMAT(1X,8F15.6)	0012
4	FORMAT(1X,12I10)	0013
5	FORMAT(1H0)	0014
	IDC=30	0015
	IDH=400	0016
	IDJ=150	0017
	IDZ=465	0018
20	AL=18.7325	0019
	BL=19.05	0020
	ER=3.	0021
	DPH=2.	0022
	PHA=0.54	0023
	PHB=14.8	0024
	PHC=PHB	0025
	IF(PHA.GT.PHB)PHA=PHB	0026
	IF(PHC.GT.PHB)PHC=PHB	0027
	N=.5+(SQRT(1.+8.*IDZ)-1.)/2.	0028
	IF(N.LT.IDC)IDC=N	0029
	NN=IDC	0030
	SQR=SQRT(ER)	0031
	ETA1=ETA/SQR	0032
	TL=BL-AL	0033
	WRITE(6,2)AL,BL,TL,ER,PHA,PHB,PHC	0034
	WRITE(6,5)	0035
	AK=TP*AL	0036
	BK=TP*BL	0037
	AK1=AK*SQR	0038
	BK1=BK*SQR	0039
	PHAR=.0174533*PHA	0040
	PHBR=.0174533*PHB	0041
	PHCR=.0174533*PHC	0042
	GNU=PI/PHBR	0043
30	CALL BESSI(AK1,GNU,AJJ,AYY,AJP,AYP,IDJ,IDH,KK, BB,YY)	0044
	CALL BESSI(BK1,GNU,BJ1,BY1,BJP1,BYP1,IDJ,IDH,LL, BB,YY)	0045
	CALL BESSI(BK,1.,BB,YY,BP,YP,IDH,IDH,II, BB,YY)	0046
	IF(LL.LT.KK)KK=LL	0047
	KMIN=BK*PHB/180.	0048
	IMIN=BK	0049
	NMIN=BK*PHC/180.	0050
	NMAX=.5+KK*PHC/PHB	0051
	IF(NN.GT.IDC)NN=IDC	0052
	IF(NN.GT.NMAX)NN=NMAX	0053
	IF(NN.LT.1)NN=1	0054
	WRITE(6,4)IMIN,II,KMIN,KK,NMIN,NN	0055
	WRITE(6,5)	0056
	SUMN=(.0,.0)	0057
	BHR(1)=CMPLX(BB(1),-YY(1))/CMPLX(BP(1),-YP(1))	0058
	DO 60 I=2,11	0059
	BHR(I)=CMPLX(BB(I),-YY(I))/CMPLX(BP(I),-YP(I))	0060
	N=I-1	0061
	SC=SIN(N*PHCR)/(N*PHCR)	0062

Fig. 7. The MAIN computer program.

	SNC(I)=SC	0063
60	SUMN=SUMN+BHR(I)*SC*SC	0064
	RUM1=AJP(1)*BY1(1)-BJ1(1)*AYP(1)	0065
	REN1=AJP(1)*BYP1(1)-BJP1(1)*AYP(1)	0066
	SUML=.0	0067
	SUMP=.0	0068
	DO 70 K=2, KK	0069
	BEN(K)=AJP(K)*BYP1(K)-BJP1(K)*AYP(K)	0070
	RBES(K)=(AJP(K)*BY1(K)-BJ1(K)*AYP(K))/BEN(K)	0071
	GNU=(K-1.)*PI/PHBR	0072
	SC=SIN(GNU*PHCR)/(GNU*PHCR)	0073
	SGC(K)=SC	0074
	SGA(K)=SIN(GNU*PHAR)/(GNU*PHAR)	0075
	SUMP=SUMP+SGA(K)*SC/BEN(K)	0076
70	SUML=SUML+RBES(K)*SC*SC	0077
	Z(1)=ETA1*PHBR*(.5*BHR(1)+SUMN)/(ETA*PI)-.5*RUM1/REN1-SUML	0078
	Z(1)=PHCR*Z(1)	0079
	V(1)=CMPLX((1./REN1+2.*SUMP)/(AK*BK1),0.)	0080
	IF(NN.EQ.1)GO TO 130	0081
	DO 120 N=1, NN	0082
	MA=2	0083
	IF(N.GT.2)MA=N	0084
	DO 120 M=MA, NN	0085
	SJN=(.0,.0)	0086
	DO 100 I=2, II	0087
	CALL GNJ(I, M, PHCR, SNC, GIM)	0088
	GIN=SNC(I)	0089
	IF(N.GT.1)CALL GNJ(I, N, PHCR, SNC, GIN)	0090
100	SJN=SJN+BHR(I)*GIM*GIN	0091
	SJL=.0	0092
	CJR=.0	0093
	DO 110 K=2, KK	0094
	CALL GLJ(K, M, PHBR, PHCR, SGC, FKM)	0095
	FKN=SGC(K)	0096
	IF(N.GT.1)CALL GLJ(K, N, PHBR, PHCR, SGC, FKN)	0097
	IF(N.EQ.1)CJR=CJR+FKM*SGA(K)/BEN(K)	0098
110	SJL=SJL+RBES(K)*FKM*FKN	0099
	L=(N-1)*NN-(N*N-N)/2+M	0100
	Z(L)=(ETA1*PHBR*SJN)/(ETA*PI)-SJL*PHCR	0101
120	IF(N.EQ.1)V(M)=CMPLX(2.*CJR/(AK*BK1),0.)	0102
130	CALL SOROT(Z, V, 0, 1, NN)	0103
	A(1)=-(.0,1.)*PHCR*B(1)/(ETA*PI*CMPLX(BP(1),-YP(1)))	0104
	DO 300 I=2, II	0105
	SC=SNC(I)	0106
	SUL=B(1)*SC	0107
	IF(NN.EQ.1)GO TO 300	0108
	DO 290 N=2, NN	0109
	CALL GNJ(I, N, PHCR, SNC, GIN)	0110
290	SUL=SUL+B(N)*GIN	0111
300	A(1)=-2.*PHCR*(.0,1.)*SUL/(ETA*PI*CMPLX(BP(1),-YP(1)))	0112
	C(1)=(.0,1.)*(2.*AL*PHCR*B(1)*AYP(1)-BYP1(1))/	0113
	2(2.*AL*ETA1*PHBR*REN1)	0114
	D(1)=(.0,1.)*(BJP1(1)-2.*AL*PHCR*B(1)*AJP(1))/	0115
	2(2.*AL*ETA1*PHBR*REN1)	0116
	DO 340 K=2, KK	0117
	SA=SGA(K)	0118
	REN=AL*ETA1*PHBR*BEN(K)	0119
	SUL=B(1)*SGC(K)	0120
	IF(NN.EQ.1)GO TO 330	0121
	DO 320 N=2, NN	0122
	CALL GLJ(K, N, PHBR, PHCR, SGC, FKM)	0123
320	SUL=SUL+B(N)*FKN	0124

Fig. 7.

330	C(K)=-SA*BYP1(K)+2.*AL*PHCR*AYP(K)*SUL	0125
	C(K)=(.0,1.)*C(K)/REN	0126
	D(K)=SA*BJP1(K)-2.*AL*PHCR*AJP(K)*SUL	0127
340	D(K)=(.0,1.)*D(K)/REN	0128
	Y11=C(1)*AJJ(1)+D(1)*AYY(1)	0129
	DO 360 K=2, KK	0130
360	Y11=Y11+(C(K)*AJJ(K)+D(K)*AYY(K))*SGA(K)	0131
	WRITE(6,2)Y11	0132
	WRITE(6,5)	0133
	GG=REAL(Y11)	0134
	NPH=180./DPH+1.5	0135
	DO 400 L=1,NPH	0136
	PH=(L-1)*DPH	0137
	PHR=.0174533*PH	0138
	HZ=(.0,.0)	0139
	CQ=(1,.0)	0140
	DO 390 I=1,11	0141
	N=I-1	0142
	HZ=HZ+CQ*A(1)*COS(N*PHR)	0143
390	CQ=CQ*(.0,1.)	0144
	HAB=CABS(HZ)/PI	0145
	GAIN=TP*ETA*HAB*HAB/GG	0146
	DB=10.*ALOG10(GAIN)	0147
400	WRITE(6,2)PH,GAIN,DB	0148
	CALL EXIT	0149
	END	0150

Fig. 7.

APPENDIX II SUBROUTINE BESSI

The subroutines are listed in Figs. 8-11. BESSI is a drastically modified and streamlined version of a program developed by Nelson Ma of the Department of Engineering Mechanics at The Ohio State University. This program calculates Bessel and Neumann functions and their derivatives. The argument must be positive and real. The order is positive and real, and it may be integer or noninteger. For the gamma function, BESSI calls subroutine GAMMA from the IBM 360 scientific subroutine package. The input data are defined as follows:

X argument, greater than zero
 ORD order, greater than zero
 IDL dimension of BJJ, BYY, BJP and BYP
 IDM dimension of BJ and BY

BJ and BY are work arrays for internal use. If ORD is an integer, BJ and BY may have the same names in the calling program as BJJ and BYY to reduce storage requirements. This is illustrated in the third call to BESSI in Fig. 7. The output data are defined as follows:

BJJ(I) $J_\nu(x)$ with $I = 1, 2, 3, \dots N$ and $\nu = (I - 1)*ORD$
 BYY(I) $N_\nu(x)$
 BJP(I) $J'_\nu(x)$
 BYP(I) $N'_\nu(x)$
 N maximum value of I

N will not exceed IDL. If IDL and IDM are sufficiently large, N will be determined by the condition that BJJ(N) is less than 10^{-6} or BYY(N) is greater than 10^6 . Comparison with other subroutines indicates that the output of BESSI may be accurate even when x is as large as 2000. The upper limit on x is not known.

One call to BESSI generates a series of Bessel and Neumann functions with different orders. For example, if $ORD = 0.5$ the functions will have orders 0, 1/2, 2/2, 3/2, 4/2, 5/2, etc. If $ORD = 2$, the functions will have orders 0, 2, 4, 6, etc. These are the orders required in boundary-value problems involving wedges and circular-sector cylinders.

BESSI uses the recursion techniques of Reference [5]. For x greater than 10, the phase amplitude-method is employed[6].

In line 39, the user should replace 1.E-38 with the smallest number his computer can handle without underflow. To obtain a few more Bessel and Neumann functions in the series, one may replace 1.E-6 with a smaller number in line 69, and replace 1.E6 with a larger number in line 154.

To obtain the maximum available number of Bessel and Neumann functions in the series, the required dimensions may be estimated as follows when x is greater than one:

$$IDM = 1.2 \ x + 100 - 1500/(x + 20)$$

$$IDL = IDM/ORD.$$

	SUBROUTINE BESSI(X,ORD,BJJ,BYY,BJP,BYP,IDL,IDM,N,BJ,BY)	1
	DIMENSION BJ(1),BY(1),BJJ(1),BYY(1),BJP(1),BYP(1)	2
	DATA A,PI/.577215665,3.14159265/	3
	DATA C0,C1,C2,C3,C4,C5,C6,C7,C8,C9,C10,C11,C12,C13,C14,C15,C16	4
	B,C17,C18,C19,C20,C21,C22,C23,C24,C25,C26,C27/	5
	C.25,.15625,-.375,.1171875,-1.15625,1.875,.952148438E-1,	6
	D-2.38671875,14.2265625,-19.6875,-.809326172E-1,-4.10058593,	7
	E58.2246094,-277.875,354.375,.416666667E-1,-.25,.0125,-.35,	8
	F.558035718E-3,-.424107143,3.60267857,-5.625,.30381944E-2,	9
	G-.486111111,10.2864583,-58.,78.75/	10
	J=0	11
	IF(X.LE.0.)GO TO 1	12
	IF(ORD.LE.0.)GO TO 1	13
	GO TO 2	14
1	N=J-1	15
	RETURN	16
2	EA=2./X	17
	INT=ORD+.5	18
	IN=1000.*(ORD-INT)	19
	TLOG=ALOG(X/2.)	20
	PIH=2./PI	21
	T2=1./(X*X)	22
	PI4=4./PI	23
	GAMM1=PIH*(A+TLOG)	24
	KMAX=X+10.*(2.*X**.333333+1.)	25
	SQPX=SQRT(.5*PI*X)	26
	TPX=2./(PI*X)	27
10	J=J+1	28
	JM=J-1	29
	FNUP=JM*(URU	30
	N=FNUP	31
	FNU=FNUP-N	32
	IF(IN.EQ.0)FNU=.0	33
	IF(IN.EQ.0)N=1	34
	NP1=N+1	35
	IF(NP1.GT.IDM)GO TO 1	36
	NM1=N-1	37
	K=KMAX	38
	IF(K.LT.NP1 .AND. IN.NE.0)GO TO 1	39
	I=K	40
	BJC=.0	41
	BJB=1.E-38	42
	EB=EA*(1+FNU)	43
35	BJA=EB*BJB-BJC	44
	IF(1.LE.IDM)BJ(1)=BJA	45
	EB=EB-EA	46
	BJC=BJB	47
	BJB=BJA	48
	I=I-1	49
	IF(I.GE.1)GO TO 35	50
	IF(K.GT.IDM)K=IDM	51
	M=(K-1)/2	52
	IF(X.GE.10.)GO TO 59	53
	PHI=FNU+2.	54
	MO=3	55
	ALF=PHI*BJ(3)+BJ(1)	56
	DO 39 I=2,M	57
	MO=MO+2	58
	FM2=2*I	59
	FM1=I-1	60
	F1=1	61
	TEMP=((FNU+FM2)*(FNU+FM1))/(F1*(FNU+FM2-2.0))*PHI	62

Fig. 8. Subroutine BESSI.

	PHI=TEMP	63
39	ALF=PHI*BJ(MO)+ALF	64
	GAMM=GAMMA(FNU+1.)	65
	ALF=EA**FNU*GAMM*ALF	66
41	AJ1=1.	67
	AJ2=1.	68
	JAN=0	69
	RALF=1./ALF	70
	DO 43 1=1,K	71
	IF(JAN.EQ.1)GO TO 43	72
	IF(AJ1.LT.1.E-6 .AND. AJ2.LT.1.E-6)JAN=1	73
	BJ(1)=BJ(1)*RALF	74
	AJ1=AJ2	75
	AJ2=ABS(BJ(1))	76
	IMX=1	77
43	CONTINUE	78
	K=IMX	79
	M=(K-1)/2	80
	IF(IN.NE.0 .AND. IMX.LT.NP1)GO TO 1	81
	GO TO 100	82
59	KOUNT=1	83
	GNU=FNU	84
61	AL1=GNU**2-.25	85
	A2 =C0*AL1	86
	A4=(C1*AL1+C2)*AL1	87
	A6=((C3*AL1+C4)*AL1+C5)*AL1	88
	A8=((C6*AL1+C7)*AL1+C8)*AL1+C9)*AL1	89
	A10=((C10*AL1+C11)*AL1+C12)*AL1+C13)*AL1+C14)*AL1	90
	B=((A10*T2+A8)*T2+A6)*T2+A4)*T2+A2	91
	BNU=B*T2+1.0	92
	ANU=BNU/SQPX	93
	A2=.5*AL1	94
	A4=(C15*AL1+C16)*AL1	95
	A6=((C17*AL1+C18)*AL1+.75)*AL1	96
	A8=((C19*AL1+C20)*AL1+C21)*AL1+C22)*AL1	97
	A10=((C23*AL1+C24)*AL1+C25)*AL1+C26)*AL1+C27)*AL1	98
	B=((A10*T2+A8)*T2+A6)*T2+A4)*T2+A2	99
	TPHI=B*T2+1.0	100
	PHI=TPHI*X-(GNU+.5)/PIH	101
	F1=ANU*COS(PHI)	102
	Y1=ANU*SIN(PHI)	103
	IF(KOUNT.GT.1)GO TO 65	104
	FSAVE=F1	105
	BY(1)=Y1	106
	GNU=FNU+1.0	107
	KOUNT=2	108
	GO TO 61	109
65	F2=F1	110
	BY(2)=Y1	111
	F1=FSAVE	112
	ALF=BJ(2)/F2	113
	IF(ABS(F1).GT.ABS(F2))ALF=BJ(1)/F1	114
	GO TO 41	115
100	IF(X.GE.10.)GO TO 150	116
	ARG=FNU*PI	117
	GARG=GAMM**2	118
	IF(FNU.EQ.0.)GO TO 116	119
	TERM=(1./PI)*EA**(2.*FNU)	120
	GAM1=COS(ARG)/SIN(ARG)-TERM*(GARG/FNU)	121
	GAM2=2.0*TERM*GARG*(FNU+2.0)/(1.0-FNU)	122
	GO TO 117	123
116	GAM1=GAMM1	124

Fig. 8.

```

      GAM2=PI4
117 BY(2)=-((1./PI)*BJ(1)*EA**((1.+2.*FNU)*GARG+(GAM1-GAM2/2.)*BJ(2))
      YNU=GAM1*BJ(1)
      TXNU=3.0*FNU/X
      AB=ABS(BJ(1))-0.000005
      MP1=M+1
      I2=1
      DO 121 I=2,MP1
      I2=I2+2
      FI=I
      FIM=I-1
      FI2=2*I
      DENOM=FI*(FI-FNU)*(FNU+FI2-2.0)
      GAM3=(FNU+FI2)*((2.0*FNU+FIM)*(FNU+FIM)/DENOM
      GAM3=-GAM3*GAM2
      YNU=GAM2*BJ(I2)+YNU
      IF(AB.GT.0.)GO TO 120
      E1=TXNU*GAM2
      BY(2)=E1*BJ(I2)+BY(2)
      IF(I2.GE.K)GO TO 130
      E1=(GAM2-GAM3)/2.
      BY(2)=E1*BJ(I2+1)+BY(2)
120 GAM1=GAM2
121 GAM2=GAM3
130 BY(1)=YNU
      IF(AB.GT.0.)BY(2)=(YNU*BJ(2)-TPX)/BJ(1)
150 JAN=0
      ABY=ABS(BY(2))
      MAX=NM1
      IF(IN.EQ.0)MAX=K
      DO 160 I=1,MAX
      IF(JAN.EQ.1)GO TO 160
      IMX=I+2
      IF(ABY.GT.1.E6)JAN=1
      BY(I+2)=EA*((1+FNU)*BY(I+1)-BY(I))
      ABY=ABS(BY(I+2))
160 CONTINUE
      IF(IN.EQ.0)GO TO 300
      IF(IMX.LT.NP1)GO TO 1
      BJJ(J)=BJ(NP1)
      BYY(J)=BY(NP1)
      IF(J.GT.1)GO TO 210
      BJP(1)=-BJ(2)
      BYP(1)=-BY(2)
      GO TO 220
210 FAC=FNU/X
      BJP(J)=-FAC*BJ(NP1)+BJ(N)
      BYP(J)=-FAC*BY(NP1)+BY(N)
220 IF(J.LT.IDL)GO TO 10
      N=J
      RETURN
300 BJJ(1)=BJ(1)
      BYY(1)=BY(1)
      BJP(1)=-BJ(2)
      BYP(1)=-BY(2)
      N=K
      IF(IMX.LT.K)N=IMX
      N=1+(N-1)/INT
      IF(N.GT.IDL)N=IDL
      DO 350 I=2,N
      L=1+(I-1)*INT
      LM=L-1

```

Fig. 8.

BJJ(I)=BJ(L)	187
BYI(I)=BY(L)	188
FAC=LM/X	189
BJP(I)=-FAC*BJ(L)+BJ(LM)	190
350 BYP(I)=-FAC*BY(L)+BY(LM)	191
RETURN	192
END	193

Fig. 8.

	SUBROUTINE SQROT(C,S,IWR,I12,NEQ)	0001
	COMPLEX C(1),S(1),SS	0002
2	FORMAT(1X,I15,1F10.3,1F15.7,1F10.0,2F15.6)	0003
3	FORMAT(1H0)	0004
	N=NEQ	0005
	IF(I12.EQ.2)GO TO 20	0006
	C(1)=CSQRT(C(1))	0007
	DO 4 K=2,N	0008
4	C(K)=C(K)/C(1)	0009
	DO 10 I=2,N	0010
	IMO=I-1	0011
	IPO=I+1	0012
	ID=(I-1)*N-(1*I-I)/2	0013
	II=ID+1	0014
	DO 5 L=1,IMO	0015
	LI=(L-1)*N-(L*L-L)/2+I	0016
5	C(II)=C(II)-C(LI)*C(LI)	0017
	C(II)=CSQRT(C(II))	0018
	IF(IPO.GT.N)GO TO 10	0019
	DO 8 J=IPO,N	0020
	IJ=ID+J	0021
	DO 6 M=1,IMO	0022
	MD=(M-1)*N-(M*M-M)/2	0023
	MI=MD+I	0024
	MJ=MD+J	0025
6	C(IJ)=C(IJ)-C(MJ)*C(MI)	0026
8	C(IJ)=C(IJ)/C(II)	0027
10	CONTINUE	0028
20	S(1)=S(1)/C(1)	0029
	DO 30 I=2,N	0030
	IMO=I-1	0031
	DO 25 L=1,IMO	0032
	LI=(L-1)*N-(L*L-L)/2+I	0033
25	S(L)=S(L)-C(LI)*S(L)	0034
	II=(I-1)*N-(1*I-I)/2+I	0035
30	S(I)=S(I)/C(II)	0036
	NN=(N+1)*N/2	0037
	S(N)=S(N)/C(NN)	0038
	NMO=N-1	0039
	DO 40 I=1,NMO	0040
	K=N-I	0041
	KPO=K+1	0042
	KD=(K-1)*N-(K*K-K)/2	0043
	DO 35 L=KPO,N	0044
	KL=KD+L	0045
35	S(K)=S(K)-C(KL)*S(L)	0046
	KK=KD+K	0047
40	S(K)=S(K)/C(KK)	0048
	IF(IWR.LE.0) GO TO 100	0049
	WRITE(6,3)	0050
	CNOR=.0	0051
	DO 50 I=1,N	0052
	SA=CABS(S(I))	0053
50	IF(SA.GT.CNOR)CNOR=SA	0054
	IF(CNOR.LE.0.)CNOR=1.	0055
	DO 60 I=1,N	0056
	SS=S(I)	0057
	SA=CABS(SS)	0058
	SNOR=SA/CNOR	0059
	PH=.0	0060
	IF(SA.GT.0.)PH=57.29578*ATAN2(AIMAG(SS),REAL(SS))	0061
60	WRITE(6,2)I,SNOR,SA,PH,SS	0062

Fig. 9. Subroutine SQROT.

```
WRITE(6,3)
100 RETURN
END
```

```
0063
0064
0065
```

Fig. 9.

SUBROUTINE GLJ(LL,JJ,PHBR,PHCR,SGC,FLJ)	0001
DIMENSION SGC(150)	0002
DATA PI/3.14159/	0003
J=JJ-1	0004
SGJ=(-1)**J	0005
L=LL-1	0006
FLJ=.5	0007
GNU=L*PI/PHBR	0008
SC=SGC(LL)	0009
GNUS=GNU*GNU	0010
TEST=ABS(GNU-J*PI/PHCR)	0011
DEN=GNUS-(J*PI/PHCR)**2	0012
IF(TEST.GT..001)FLJ=SGJ*GNUS*SC/DEN	0013
RETURN	0014
END	0015

Fig. 10. Subroutine GLJ.

SUBROUTINE GNJ(M,JJ,PHCR,SNC,FNJ)	0001
DIMENSION SNC(150)	0002
DATA PI/3.14159/	0003
J=JJ-1	0004
SGJ=(-1)**J	0005
N=M-1	0006
NS=N*N	0007
SC=SNC(M)	0008
FNJ=.5	0009
TEST=ABS(N-J*PI/PHCR)	0010
DEN=NS-(J*PI/PHCR)**2	0011
IF(TEST.GT..001)FNJ=SGJ*NS*SC/DEN	0012
RETURN	0013
END	0014

Fig. 11. Subroutine GNJ.

APPENDIX III SUBROUTINE SQROT

This subroutine considers the matrix equation $ZI = V$ which represents a system of simultaneous linear equations. If the square matrix Z is symmetric, SQROT is useful for obtaining the solution I with V given. NEQ denotes the number of simultaneous equations and the size of the matrix Z .

On entry to SQROT, S is the excitation column V . On exit, the solution I is stored in S . Let $Z(I,J)$ denote the symmetric square matrix. On entry to SQROT, the upper-right triangular portion of $Z(I,J)$ is stored by rows in $C(K)$ with

$$(37) \quad K = (I - 1)*NEQ - (I*I - I) / 2 + J.$$

If $I12 = 1$, SQROT will transform the symmetric matrix into the auxiliary matrix (implicit inverse), store the result in $C(K)$ and use the auxiliary matrix to solve the simultaneous equations. If $I12 = 2$, this indicates that $C(K)$ already contains the auxiliary matrix.

The transformation from the symmetric matrix to the auxiliary matrix is programmed above statement 10, and the solution of the simultaneous equations is programmed in statements 20 to 40. If IWR is positive, the program below statement 40 will write the solution.

SQROT uses the square root method described in Reference [4]. The original symmetric matrix Z and the upper triangular auxiliary matrix A are related by

$$(38) \quad Z = A' A$$

where A' is the transpose of A .

The determinant of the symmetric matrix Z may be obtained by squaring the product of the diagonal elements in the auxiliary matrix.

SQROT was developed by Dr. Robert G. Wickliff Jr., now with Hewlett Packard, Colorado Springs, Colorado 80907.

ACKNOWLEDGMENT

The experimental data presented herein were measured by Melvin C. Gilreath at NASA Langley Research Center. His kind permission to reproduce these antenna patterns is truly appreciated.